

Activity of gold catalysts in the liquid-phase oxidation of *o*-hydroxybenzyl alcohol

C. Milone, R. Ingoglia, A. Pistone, G. Neri, and S. Galvagno *

Università di Messina, Dipartimento di Chimica Industriale e Ingegneria dei Materiali, Salita Sperone 31, I-98166 Messina, Italy

Received 29 October 2002; accepted 11 February 2003

Gold catalysts prepared by impregnation of HAuCl_4 on Fe_2O_3 , ZnO , CaO , and Al_2O_3 and aged in a solution of Na_2CO_3 (IWI/ Na_2CO_3 method) are able to catalyze the oxidation of *o*-hydroxybenzyl alcohol (salicylic alcohol) under mild conditions. The reaction rate is even higher than that using analogous catalysts prepared by co-precipitation. Salicylic aldehyde is the main reaction product with a selectivity >90% at 90% conversion. The influence of the reaction conditions on the catalytic activity is also discussed.

KEY WORDS: gold catalysts; impregnation; liquid-phase oxidation; salicylic alcohol; salicylic aldehyde.

1. Introduction

A recent review dealing with the latest advances in the catalysis research on gold has pointed out that, up to now, studies have been mainly focused on the activity of gold-supported catalysts in CO oxidation and other reactions of industrial importance such as epoxidation of propylene and the water–gas shift (WGS) reaction. The use of gold catalysts for the synthesis of fine chemicals has received much less attention [1].

Recently it was demonstrated that gold-supported catalysts can be successfully employed for the selective hydrogenation of α,β -unsaturated aldehydes to α,β -unsaturated alcohols [2–6], gold being much more selective than analogous Pt catalysts [4,6].

Prati and Rossi have reported that in the oxidation of vicinal diols, ethane diols, and propan-1,2-diol, Au/C catalyst is much more selective than Pt/C and Pd/C toward the formation of the α -hydroxy acids (glycolic acid and lactic acid) [7]. The authors have also demonstrated that gold catalysts are much more stable than Pt and Pd under reaction conditions. The lifetimes of Pt and Pd catalysts are reduced by leaching, fouling, and oxidation of the noble metals.

In a previous work we reported the preliminary results of a study on the liquid-phase oxidation of *o*-hydroxybenzyl alcohol (salicylic alcohol) on Au supported on Fe_2O_3 under mild conditions ($T_r = 323\text{ K}$, in O_2 or air at $P = 1\text{ atm}$, and water as solvent) [8]. This process is of particular interest for the preparation of *o*-hydroxybenzaldehyde (salicylic aldehyde) which can be used as an intermediate for the preparation of perfumes, pesticides, chelating agents, etc. The processes for the

manufacture of *o*-hydroxybenzaldehyde are mainly chemical (Reimer–Tiemann process, formylations or carbonylation of phenol) rather than catalytic [9–11]. However, all these processes have one or more of the following disadvantages: formation of isomers that are difficult to separate, multistage synthesis, low yield, formation of large amounts of waste.

The catalytic routes for the synthesis of *o*-hydroxybenzaldehyde are mainly covered by patent. They are based on the oxidation of *o*-hydroxybenzyl alcohol by oxygen gas, in alkaline medium, on Pt- or Pd-based catalysts in the presence of modifiers such as lead or bismuth which avoids the formation of large amounts of tar improving the lifetime of the catalysts [12–14].

Christidis and Vallejos claim the disclosure of a process for the preparation of *o*- and *p*-hydroxybenzaldehydes by oxidation of *o*- and *p*-hydroxybenzyl alcohols, respectively, by oxygen gas ($P = 8\text{ atm}$), in aqueous alkaline medium ($\text{pH} > 13$), and in the presence of Cu(II), Co(II), Fe(III), Ni(II), and Mn(II) salts [15]. The maximum selectivity toward the formation of *o*-hydroxybenzaldehyde was 84% at 100% conversion of *o*-hydroxybenzyl alcohol.

In our preliminary study on the oxidation of *o*-hydroxybenzyl alcohol on Au/ Fe_2O_3 catalysts prepared by co-precipitation we found that the catalytic activity increases with the gold content and it is mainly related to the reducibility of the catalysts. Moreover, on the catalysts with low gold content (<1 wt%) the selectivity toward the formation of salicylic aldehyde is 90% at up to 100% conversion [8]. On increasing the gold content the yield of salicylic aldehyde decreases with the conversion level and it was demonstrated that high levels of organic by-products are recovered on the catalytic surface [8].

Because of the encouraging results in terms of selectivity toward the formation of salicylic aldehyde

* To whom correspondence should be addressed.
E-mail: galvagno@ingegneria.unime.it

obtained in the previous study on low-loaded Au catalysts, we decided to carry out a systematic study on the influence of the preparation method, the nature of the support, and the reaction conditions on the catalytic activity of gold catalysts in the liquid-phase oxidation of salicylic alcohol.

2. Experimental

Gold catalysts supported on Fe₂O₃, ZnO, CaO, and Al₂O₃, with a nominal gold content of 2 wt%, were prepared by wetness impregnation of the support with an aqueous solution of HAuCl₄ (Fluka). The resulting materials were dried under vacuum at 353 K. Subsequently, solids were suspended into an aqueous solution of 1 M Na₂CO₃ and after 30 min of stirring at 323 K the impregnated samples were filtered, washed with deionized water, and then dried under vacuum at 353 K for one day. This preparation method has been named IWI/Na₂CO₃. The gold content was determined as described previously [8].

The iron oxide (Fe₂O₃) and zinc oxide (ZnO) supports were prepared by precipitation of the hydroxides by adding, respectively, Fe(NO₃)₃·9H₂O to an aqueous solution of 1 M Na₂CO₃ and Zn(NO₃)₂ to an aqueous solution of 1 M NaOH and kept under vigorous stirring at a temperature of 353 K. The precipitate was digested overnight at room temperature, washed several times with water, and then dried under vacuum at 353 K. CaO and Al₂O₃ supports were commercial products.

Surface area measurements were made using the BET nitrogen adsorption method in a conventional volumetric apparatus, after outgassing (10^{−4} mbar) the sample at 353 K for 2 h.

X-ray diffraction (XRD) studies were carried out using an Ital-Structures diffractometer using nickel-filtered CuKα radiation by mounting the powder samples on plexiglas holders. Diffraction peaks were compared with those reported in the JCPDS Data File.

Temperature-programmed reduction (TPR) experiments were carried out using a conventional apparatus. The sample (weight = 0.05 g) was heated from room temperature to 800 K (heating rate 10 K/min) under 5% H₂/Ar (vol%) with a constant flow rate of 20 cm³/min. A molecular sieve cold trap (maintained at 193 K) and a tube filled with KOH were used to block water and CO₂, respectively, before the thermal conductivity detector (TCD).

Catalytic experiments were carried out at atmospheric pressure under O₂ flow, at 323 K, in a 100 ml four-necked batch reactor fitted with a reflux condenser, dropping funnel, thermocouple, and magnetic stirrer head coupled with a gas stirrer (model MRK 1/20-BR purchased from Premex Reactor) to optimize the oxygen transfer from the gas to the liquid phase. The catalyst (0.5 g; particle size 50–75 μm) was added to 25 ml of solvent and treated

at 323 K for 10 min under gaseous O₂. The substrate (5.5 × 10^{−4} mol) was injected through one arm of the flask. The reaction mixture was stirred at 500 rpm.

The *o*-hydroxybenzyl alcohol was a commercial analytical product (Fluka, assay 99%).

The progress of the reaction was followed by sampling a sufficient number of microsamples and analyzing them by HPLC (Waters model 510) equipped with a photodiode array detector (PAD; Waters 996).

The reaction products were separated on a Symmetry C18 column (5 μm, 4.6 × 250 mm), using a water/acetonitrile solution (gradient method). The total flow was kept at 0.8 ml/min. Calibration curves for the reagent and reaction products were obtained by analyzing reference samples under the above reported experimental conditions. *o*-Hydroxybenzyl alcohol was detected at 273.4 nm, *o*-hydroxybenzaldehyde at 212.2 nm, and *o*-hydroxybenzoic acid (salicylic acid) at 202.8 nm. Data acquisition and processing were carried out using Millennium³² software version 4.0.

Preliminary runs carried out with different stirring conditions, amount of catalyst, and catalyst grain size have shown the absence of external and internal diffusional limitations.

3. Results and discussion

3.1. Characterization of gold preparations

The chemical composition and the surface area (SA) of the gold preparations and of the parent supports are reported in table 1. It can be seen that gold catalysts supported on Fe₂O₃ and Al₂O₃ have a SA very close to that of the parent supports. A drastic SA decrease is instead observed from ZnO to the AuZn catalyst whereas a reverse trend with respect to the parent support, *i.e.* an increase of the SA, has been obtained on AuCa catalyst.

The gold loading of the Au samples ranges between 1.2 and 1.7 wt%. Considering that 2 wt% was the

Table 1
Main characteristics of gold-supported catalysts and of the parent supports

| Code | Au (wt%) | SA (m ² /g) | Au particle size ^a (nm) |
|--------------------------------|----------|------------------------|------------------------------------|
| CaO | – | 3 | – |
| AuCa | 1.2 | 11 | 25.7 |
| Fe ₂ O ₃ | – | 178 | – |
| AuFe | 1.4 | 176 | 46.6 |
| ZnO | – | 20 | – |
| AuZn | 1.7 | 4 | 35.4 ^b |
| Al ₂ O ₃ | – | 120 | – |
| AuAl | 1.3 | 121 | 13.4 |

^a Measured by XRD.

^b Measured on the used catalyst after one run.

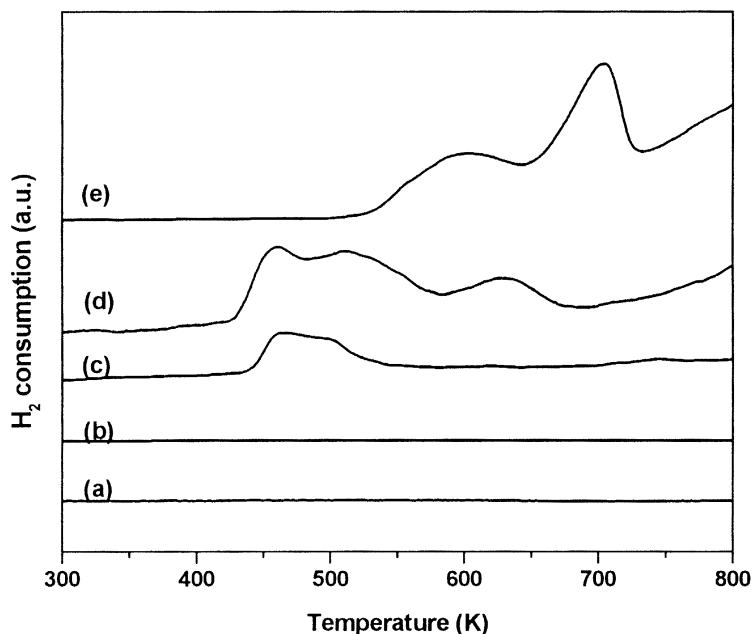


Figure 1. TPR profiles of gold-supported catalysts. (a) AuAl; (b) AuCa; (c) AuZn; (d) AuFe; (e) Fe₂O₃.

nominal Au content, the noble metal lost ranges between 15 and 40%. These values are much lower than the 80% lost reported for gold catalysts prepared by co-precipitation or deposition–precipitation at high pH [16].

No correlation can be drawn between the surface area of the solids and the gold deposited on the prepared samples (table 1). It can be argued that, in our case, the yield of deposition of gold is high because during the impregnation step the gold precursor is strongly anchored on the surface of the support and this interaction prevents dissolution during aging in Na₂CO₃. This conclusion is supported by previous ¹⁹⁷Au Mössbauer spectroscopy, TPR, and XRD studies on Au/Fe₂O₃ catalysts prepared by conventional impregnation of the support with a solution of HAuCl₄ and dried at 353 K [17,18]. All the characterization techniques agree with the presence of gold species such as Au(III) oxychlorides formed by interaction of the HAuCl₄ precursor with the surface of iron oxide. No evidence of HAuCl₄ on the support was obtained.

TPR profiles of the investigated catalysts are shown in figure 1. AuAl and AuCa catalysts do not show H₂ consumption over the range of temperature investigated, thus indicating that on the end solids gold is mainly present in a metallic state (figures 1(a) and 1(b)). On AuZn a reduction peak at low temperature, $T_{\max} = 450$ K, was observed (figure 1(c)). It has to be mentioned that in the absence of gold, ZnO support does not show any reduction peak in the range of temperature investigated. The estimation of the amount of H₂ consumed agrees with the reduction of gold from Au(III) to metallic gold. Since HAuCl₄ has been reported to reduce at 554 K [18], the low temperature at which the reduction of gold occurs suggests the presence of highly hydroxylated gold species [18,19].

In the case of AuFe several reduction peaks are observed in the range 423–673 K (figure 1(d)). For comparison the TPR profile of the support alone has been also included (figure 1(e)). The latter is composed of two overlapping peaks. The peak with $T_{\max} = 703$ K has been attributed to the Fe₂O₃ → Fe₃O₄ reduction step [18,20,21]. The shoulder at low temperature is due to the partial reduction of highly hydroxylated Fe(III) species [21]. The TPR spectra of AuFe differ substantially from that of Fe₂O₃. Two overlapping peaks are observed at lower temperature ($T_{\max 1} = 450$ K, $T_{\max 2} = 483$ K) together with a peak at 573 K. The total H₂ consumption corresponds to the reduction Fe₂O₃ → Fe₃O₄, thus indicating that also in this sample gold is present in a metallic state. In agreement with previous results reported for catalysts prepared by co-precipitation or deposition–precipitation, the temperature for the partial reduction of the support is strongly lowered upon addition of gold [18,20–24].

It is noteworthy that Au/Fe₂O₃ catalysts, having similar gold loading and prepared by classical co-precipitation or IWI/Na₂CO₃ (this work), promote the partial reduction of Fe₂O₃ → Fe₃O₄ in a similar range of temperature [18].

Considering that the enhancement of the reducibility of the support upon addition of gold has been previously ascribed to a stronger interaction between the metal and the support, which is typically obtained during co-precipitation, we can conclude that the IWI/Na₂CO₃ preparation method also allows an intimate contact between the metal and the support.

Recently Golunski *et al.* have classified as NSA (normal support activation) the formation of highly active sites being created on metal oxides by noble

metals, including gold [24]. It has been reported that the NSA effect is consistent with a “junction effect” [25] arising from contact between the support and a metal with high work function, which in turn reduces the activation energy for oxygen vacancy formation in a metal oxide. In this way, the metal promotes the reducibility of the metal oxide. The shift to lower temperature of the reduction peak of the support in the TPR profile of gold catalysts has been observed when gold is supported on highly reducible CeO_2 as well as on the less reducible ZrO_2 [26]. The role of hydrogen spillover in the promotion of the reducibility of the support was ruled out because of the inability of gold to dissociate hydrogen [26]. In our case we cannot exclude *a priori* that reduction of the support also occurs through a mechanism involving the spillover of hydrogen because gold-supported catalysts, including those used in the present work, have shown catalytic activity in the hydrogenation of α,β -unsaturated aldehydes. This is a reaction for which the activation of H_2 by the metal has to occur [6,27].

From TPR characterization it can be pointed out that the main difference between gold-supported catalysts prepared by co-precipitation and $\text{IWI}/\text{Na}_2\text{CO}_3$ is the chemical state of the noble metal. An extensive characterization of the former by means EXFAS [28], ^{197}Au Mossbauer spectroscopy [17], TPR [18], XPS [29], and FTIR [30] unequivocally suggested that on the as-prepared catalysts gold is mainly present in an oxidized state. Only a fraction of the gold is in a metallic state. On the $\text{IWI}/\text{Na}_2\text{CO}_3$ samples, however, gold is in a metallic state, with the exception of AuZn catalyst. The preferential formation of metallic gold on these samples can be explained by assuming that $\text{Au}(\text{OH})_3^-$ and

$\text{Au}(\text{OH})_4^-$ species, formed during the hydrolysis at high pH [31], are mainly distributed on the external surface of the catalysts and can more easily undergo photo and/or thermal decomposition to metallic gold. Chen and Yeh have reported that $\text{Au}(\text{III})$ supported on TiO_2 and Al_2O_3 prepared by deposition–precipitation rapidly decomposes to metallic gold under mild conditions [19]. In the case of catalysts prepared by co-precipitation, however, gold species are well mixed within the co-precipitate and are much more stabilized against decomposition to metallic gold [28].

The open question is why gold species supported on ZnO do not decompose. BET measurements, reported in table 1, show that the structure of the solid collapses during the preparation of gold catalysts; SA decreases from $20\text{ m}^2/\text{g}$ (support) to $4\text{ m}^2/\text{g}$ (AuZn). This can cause the occlusion of gold into the matrix of the ZnO preventing its decomposition to metallic gold, in a manner similar to that observed for the co-precipitated catalysts.

Structural characteristics of the gold catalysts have been investigated by XRD. The mean particle sizes of gold were determined via the Scherrer equation and are reported in table 1.

Iron oxide and Al_2O_3 supports show diffraction peaks of hematite and goethite and $\delta\text{-Al}_2\text{O}_3$, respectively. In the presence of gold an additional peak at $2\theta = 38.1^\circ$ appears, which is a typical diffraction from $\text{Au}(111)$ planes of metallic gold. The XRD spectrum of AuZn catalyst is similar to that of the parent support and no diffraction due to metallic gold was observed.

Figures 2(a) and 2(b) show the XRD spectra of calcium oxide and AuCa catalyst, respectively. The

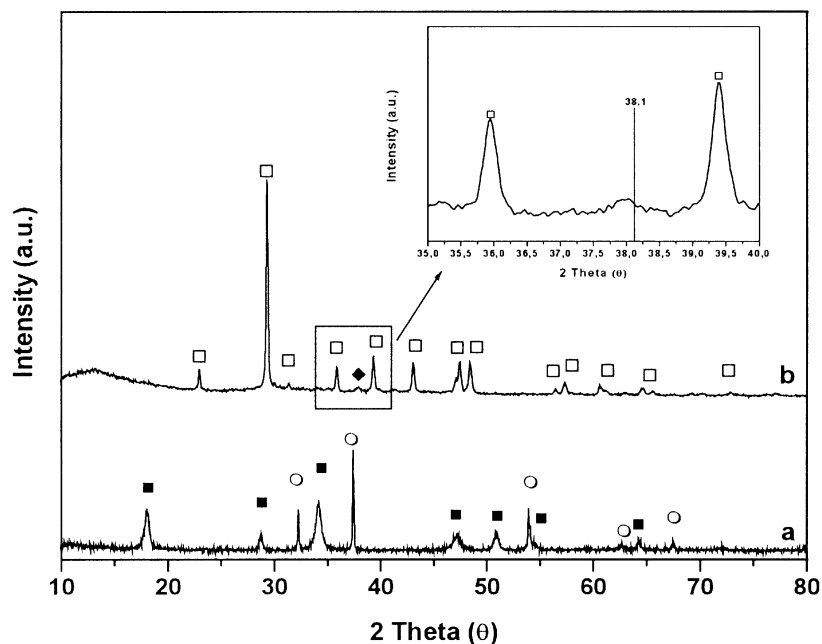


Figure 2. XRD spectra of AuCa catalyst and of the parent support. The inset is an enlargement of the region indicated: (a) CaO ; (b) AuCa . (■) Portlandite, $\text{Ca}(\text{OH})_2$; (○) lime, CaO ; (□) calcite, CaCO_3 ; (◇) metallic gold.

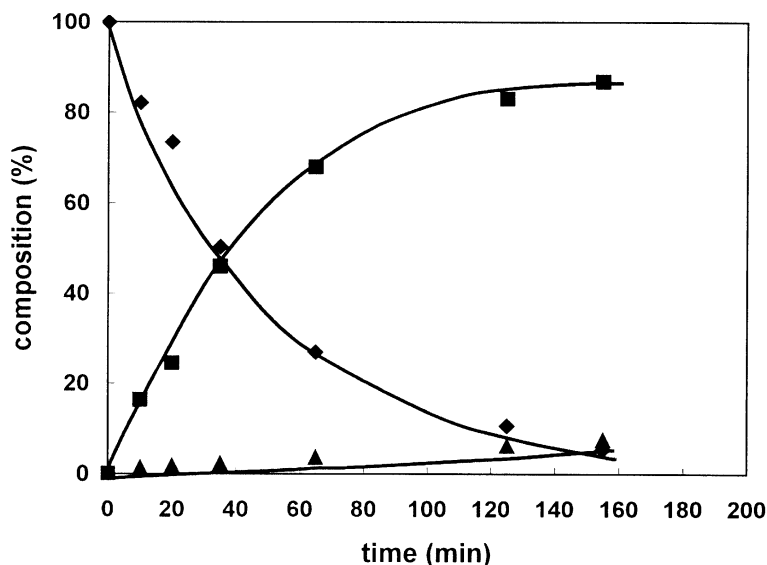


Figure 3. Typical course of the oxidation of salicylic alcohol on gold-supported catalysts. Catalyst = AuZn, weight = 0.5 g, $T_r = 323$ K, $P_{O_2} = 1$ atm, solvent = aqueous solution of 1 M Na_2CO_3 . Salicylic alcohol (◆), salicylic aldehyde (■), salicylic acid (▲).

latter shows well-resolved patterns relative to calcite, $CaCO_3$, thus indicating that during the aging in Na_2CO_3 the support undergoes a transformation from CaO and $Ca(OH)_2$ (figure 2(a)) to $CaCO_3$. In addition, a diffraction peak at $2\theta = 37.9^\circ$ was also observed. This peak cannot be attributed to residual CaO and $Ca(OH)_2$ or to $CaCO_3$, because of the absence of diffraction peaks of these compounds at that position. The distribution of gold metal particles evidenced by TEM is homogeneous and a mean diameter of 25 nm was calculated. This value agrees with that obtained by applying the Scherrer equation (table 1) to the peak at $2\theta = 37.9^\circ$ detected in the XRD spectrum. Therefore, it is likely that the diffraction peak at $2\theta = 37.9^\circ$ is due to metallic gold.

The shift to lower angle of the diffraction peak of the gold indicates that an increase of the d spacing of the lattice metallic gold occurs. The reason for the deformation of the metal lattice is unknown. It can be speculated that the increase of the d spacing is generated by a “strain effect” by the support during the transformation of the original mixture of CaO and $Ca(OH)_2$, which have a molar volume of 16.76 and 33.06 cm^3/mol , respectively, to $CaCO_3$, which has a higher molar volume of 36.90 cm^3/mol , and/or by the occlusion of “impurities” into the gold matrix. A more detailed investigation is, however, necessary to highlight the exact reason for the observation.

In summary, XRD data confirm that gold supported on Fe_2O_3 and Al_2O_3 is in a metallic state, while when it is dispersed on ZnO metallic gold is not formed, probably because it is occluded within the ZnO matrix. Moreover it is shown that on AuCa catalyst the support, originally formed by a mixture of CaO and $Ca(OH)_2$, is completely transformed into well-ordered calcite,

$CaCO_3$, during the aging in Na_2CO_3 . Gold is in a metallic state and it shows an expansion of the lattice.

3.2. Catalytic activity

The liquid-phase oxidation of salicylic alcohol has been carried out under mild conditions ($T_r = 323$ K, $P_{O_2} = 1$ atm) on all the catalysts reported in table 1. Considering that $CaCO_3$, which as demonstrated by XRD is the real support of the AuCa catalyst, is quite soluble in water ($pK_{s(298\text{ K})} = 8.7 \times 10^{-9} \text{ mol}^2/l^2$), we decided to carry out the reaction in an aqueous solution of 1 M Na_2CO_3 to reduce the solubility of calcium carbonate through the common ion effect. Moreover, to compare all the catalysts under the same conditions the basic solution has been generally adopted as the reaction medium.

The oxidation of salicylic alcohol previously carried out on the supports, in the absence of gold, does not occur under our reaction conditions. On all gold preparations, however, a strong enhancement of the catalytic activity has been observed and the oxidation of salicylic alcohol follows a first-order reaction rate law with respect to the alcohol concentration (figure 3). The main reaction products are salicylic aldehyde and salicylic acid which are formed from the oxidation of salicylic alcohol through parallel reactions.

Table 2 gives the first-order reaction rate constant K ($\text{min}^{-1} \text{ g}_{\text{cat}}^{-1}$) and selectivity toward the reaction products measured at 90% conversion. The catalytic activity ranks in the order $AuAl < AuZn < AuFe \ll AuCa$, following the increase of the basicity of the supports. Gold supported on the most basic $CaCO_3$ shows the highest catalytic activity. It is noteworthy that on the AuZn sample discharged from the reaction vessel after

Table 2
Catalytic activity of gold preparations in the liquid-phase oxidation of salicylic alcohol

| Code | Au (wt%) | Au ^a (wt%) | <i>K</i> (10 ³ min ⁻¹ g ⁻¹) | Sel. (%) (conv. = 90%) | |
|------|-------------|--------------------------|--|------------------------|------|
| | | | | Aldehyde | Acid |
| AuCa | 1.2 | 1.1 | 396 | 87.8 | 13.2 |
| AuFe | 1.4 | 1.3 | 39.5 | 87.6 | 12.4 |
| AuZn | 1.7 | 1.6 | 34.1 | 94.7 | 5.3 |
| AuAl | 1.3 | 1.2 | 8.6 | 93.1 | 6.9 |

Note: Reaction conditions: $T_r = 323$ K, $P_{O_2} = 1$ atm, solvent = aqueous solution of 1 M Na₂CO₃.

^a Measured on the used catalysts.

one run, TPR and XRD measurements show that gold is in a metallic state. The TPR profile shows the absence of the reduction peak at lower temperature, previously observed on the fresh sample (figure 1(c)), while the XRD spectra show a diffraction peak at $2\theta = 38.1^\circ$ typical of metallic gold. Therefore, it is likely that on the AuZn catalyst gold is reduced by the alcohol.

Gold catalysts show good stability under reaction conditions, as is demonstrated by the analysis of the gold content on the solid after the run. The amount of gold on the used catalysts is very close to that of the fresh samples, thus indicating that the leaching of the noble metal is almost negligible.

On all the catalysts, the partial oxidation of salicylic alcohol to salicylic aldehyde is the preferred path of reaction. The selectivity toward the formation of salicylic aldehyde is higher than 90% on the Al₂O₃ and ZnO gold-supported catalysts and it is slightly lower on AuCa and AuFe catalysts (table 2).

Catalytic experiments have clearly demonstrated that gold-supported catalysts prepared by the IWI/Na₂CO₃ method are suitable for the selective oxidation of *o*-hydroxybenzyl alcohol to *o*-hydroxybenzaldehyde, even more so than catalysts prepared by co-precipitation. It is noteworthy that, keeping the metal content constant, gold catalysts supported on iron oxide prepared by IWI/Na₂CO₃ show a higher activity than analogous samples prepared by co-precipitation [8]. Moreover, the selectivity toward the formation of *o*-hydroxybenzaldehyde is high in the entire range of conversion investigated, while on analogous catalysts prepared by co-precipitation we have observed a decrease of the selectivity toward the formation of aldehyde on increasing the conversion of alcohol [8]. This point is discussed in section 3.3.

The increase of the catalytic activity with the basicity of the support suggests that the activation of the alcohol occurs on the support through formation of an alkoxide intermediate, which is further oxidized by active oxygen species.

On Au supported on Me_xO_y catalysts (Me = Al(III), Zn(II), Fe(III)) the activation of oxygen by gold metal is unlikely to occur, because the metal particles (table 1)

are too large to account for stable adsorption of O₂ [32]. However, Choi *et al.* have reported that Au/SiO₂ catalysts prepared by conventional impregnation and treated under severe conditions (drying at 1023 K and calcination at 723 K) are able to adsorb oxygen in the atomic state under very mild conditions [33]. The authors do not report data on gold particle sizes but it is reasonable to assume that gold should not be of nanometric size, because the temperature of treatment is very close to the gold Tamman temperature. The adsorption ability of gold has been attributed to strong interaction between gold and the support or to the surface heterogeneity of the metal.

In our previous work concerning the oxidation of *o*-hydroxybenzyl alcohol on Au/Fe₂O₃ catalysts prepared by co-precipitation, it was suggested that the active oxygen species are the lattice oxygen of the support located in the outermost layers, probably at the interface between gold and the support [8]. The increase of the catalytic activity with the gold content has been correlated with the enhancement of the reducibility of the support [8]. Considering the results of the TPR investigations discussed above, where it is evidenced that the AuFe catalyst is able to promote the reduction of the support in a similar manner as does the catalyst prepared by co-precipitation, it can be argued that also in this case the oxidation of *o*-hydroxybenzyl alcohol mainly involves the lattice oxygen. The higher catalytic activity of the catalysts prepared by IWI/Na₂CO₃ compared to catalysts prepared by co-precipitation could be due to an increase of the amount of active sites exposed on the external surface of the support. It is noteworthy that co-precipitated catalysts of the previous work [8] were thermally treated under very mild conditions; therefore gold should be strongly embedded into the matrix [28], which in turn decreases the availability of the active sites.

According to the results obtained by Rajaram *et al.* [26], it can also be argued that for gold supported on the less reducible Al₂O₃ and ZnO the active oxygen species are formed at the metal-support interface. The authors reported an enhancement of the reducibility of the less reducible ZrO₂ in the presence of gold and this behavior was ascribed to the "junction effect" occurring at the metal-support interface. However, the extent of reduction of ZrO₂ is much less than that observed on the reducible CeO₂ support, and the reduction peak was detectable only upon increasing the amount of noble metal up to 4 wt% [26]. Therefore, it is likely that for our catalysts having a gold content slightly higher than 1% TPR experiments are not sensitive enough to detect the extent of reduction of the supports.

On the AuCa sample, which is the most active one, an active role of the oxygen of the support can be ruled out simply because of the chemical nature of CaCO₃, which has no mobile oxygen in the matrix. In fact, in contrast to other oxides, in this case oxygen is covalently bonded to carbon in the triangular planar CO₃²⁻ and is not available to create vacancy sites.

Therefore, on the AuCa catalyst an active role of gold in the activation of oxygen has to be taken into account to explain its catalytic activity. It has to be remembered that the XRD spectrum of this sample shows an expansion of the gold lattice which, according to Mavrikakis *et al.* [32], could be responsible for the enhancement of the reactivity of the gold surface toward the activation of O₂.

3.3. Influence of reaction conditions

The influence of the pH of the reaction medium in the liquid-phase oxidation of salicylic alcohol has been investigated. The pH was varied in the range 7–11. It was possible to study the influence of pH on the catalytic activity for all catalysts but AuCa. In fact gold catalysts supported on Al₂O₃, ZnO, and Fe₂O₃ soaked in H₂O do not modify the pH of the solvent. Therefore the reactions at different pH have been carried out using just water (pH ~7) or an aqueous solution of Na₂CO₃ having the pH of interest. In the case of AuCa, however, due to the solubility of the support, the pH of the reaction medium increases up to 10 and it cannot be decreased by addition of an acid because of thermodynamic reasons (pK_s equilibrium constant).

Table 3 gives the catalytic activity of gold preparations at different pH. It is shown that the rate of oxidation of salicylic alcohol does not depend on the pH of the reaction medium in the range investigated, thus indicating that the basicity of the solution does not influence the activation of the substrate, which mainly occurs on the surface of the solids. When the reaction is carried out at pH >8 the selectivity toward the formation of salicylic aldehyde and salicylic acid remains constant in the whole range of conversion investigated (figure 4). At lower pH, however, it was observed that,

| Code | pH of the solution at beginning of the reaction | K ($10^3 \text{ min}^{-1} \text{ g}^{-1}$) | pH of the solution at the end of the reaction |
|------|---|---|---|
| AuZn | 10.47 | 36.5 | 9.28 |
| AuZn | 8.98 | 36.1 | 8.66 |
| AuZn | 6.91 | 36.2 | 4.96 |
| AuFe | 11.05 | 39.5 | 10.60 |
| AuFe | 8.61 | 36.4 | 8.56 |
| AuFe | 6.87 | 32.2 | 4.61 |
| AuAl | 10.01 | 8.6 | 9.64 |
| AuAl | 8.92 | 7.7 | 8.97 |
| AuAl | 6.94 | 7.9 | 4.21 |

in the early stage of the reaction, the selectivity toward the formation of salicylic aldehyde is similar to that obtained at higher pH and it decreases during the course of reaction (figure 4). The selectivity toward the formation of salicylic acid, however, is similar to that observed at higher pH and it remains constant during the reaction. Therefore it can be excluded that the decrease of the salicylic aldehyde is due to its further oxidation to salicylic acid. From the decrease of the selectivity of the salicylic aldehyde no other products have been detected by HPLC analysis. This leads to a negative material balance, which progressively increases, in absolute value, during the course of the reaction. This behavior has been previously observed on Au/Fe₂O₃ catalysts prepared by co-precipitation, and it was found that the extent of the decrease of the yield to salicylic aldehyde does not depend on the gold loading when it is higher than 1 wt% [8].

Also for the catalysts investigated in this work, we have not observed any influence of the chemical or

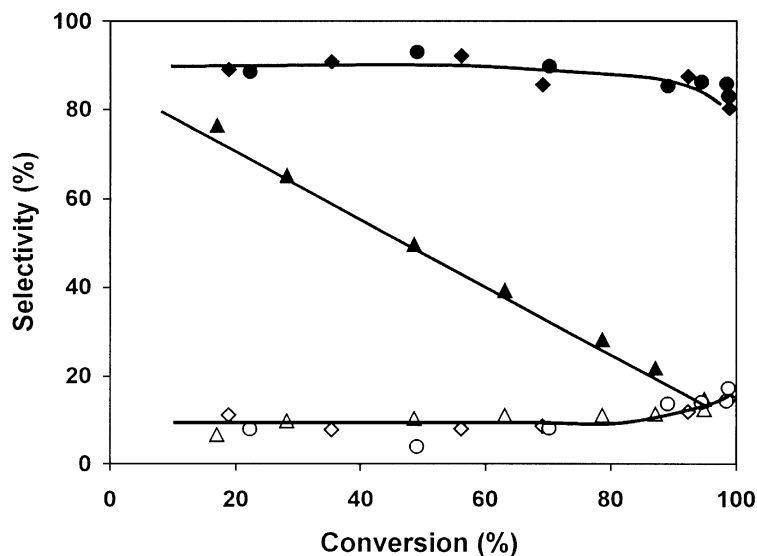


Figure 4. Product distribution in the oxidation of salicylic alcohol on AuFe as a function of conversion for reactions carried out at different pH. Salicylic aldehyde: (◆) pH = 11.05, (●) pH = 8.61, (▲) pH = 6.87; salicylic acid: (◇) pH = 11.05, (○) pH = 8.61, (△) pH = 6.87.

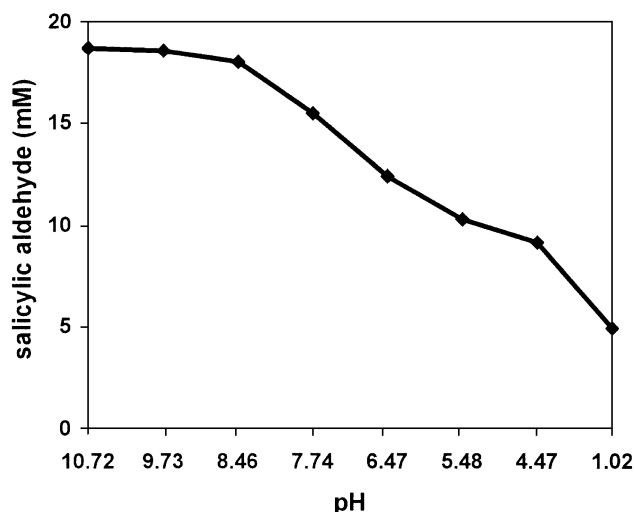


Figure 5. Concentration of salicylic aldehyde versus pH of the solution.

morphological properties of the catalysts on the extent of decrease of the yield of aldehyde.

In order to get a deeper insight into the phenomenology, we have monitored the pH of the solution during the course of reactions. It was observed that when the reaction is carried out under basic conditions, the pH remains almost constant during the run, as shown in table 3, which also gives the pH of the solution at the end of the reaction when the conversion of alcohol is 100%. Under neutral conditions the pH of the reaction medium progressively decreases during the run leading, at the end of the reaction, to an acid solution.

The decrease of the pH of the solution when the reaction is carried out under neutral conditions is obviously due to the progressive increase of the concentration of H^+ generated from the dissociation of salicylic acid, which is quite a strong acid, the first dissociation being $K_{a1(298\text{ K})} = 1.07 \times 10^{-3} \text{ mol/l}$. The constancy of the pH during the run when the reaction is carried out in a solution of Na_2CO_3 can be explained assuming a buffer effect of the couple CO_3^{2-}/HCO_3^- . Therefore it seems that the decrease of the concentration of salicylic aldehyde during the run is mainly related to the acidity of the reaction medium. A confirmation of this correlation has been obtained with a blank experiment during which the concentration of salicylic aldehyde was monitored as a function of the pH of the solution. The starting solution was an aqueous solution of salicylic aldehyde (18 mM) and Na_2CO_3 (pH = 10) and the pH was slowly decreased to 1 by addition of HCl. Figure 5 clearly shows that on decreasing the pH of the solution the concentration of the aldehyde in the solution also decreases in a similar manner as observed during the reactions.

Temperature-programmed oxidation (TPO) experiments carried out on the fresh and used catalysts have shown the presence of a single peak centered at 503 K relative to evolution of CO_2 on the used catalysts,

while the CO_2 evolved from the fresh catalysts was always negligible. Therefore it can be concluded that the disappearance of salicylic aldehyde occurs through conversion of the substrate to compounds that are adsorbed on the catalysts. The conversion of salicylic aldehyde is not catalyzed by the solids but depends on the pH of the reaction medium.

4. Conclusions

The results obtained can be summarized as follows.

- Gold catalysts prepared by wetness impregnation of the support with a solution of $HAuCl_4$ followed by aging in Na_2CO_3 (IWI/ Na_2CO_3) are more active than analogous co-precipitated catalysts for the liquid-phase oxidation of *o*-hydroxybenzyl alcohol.
- The catalytic activity depends on the basicity of the support and ranks in the order $AuAl < AuZn < AuFe \ll AuCa$.
- On all the catalysts investigated salicylic aldehyde is the main reaction product. Selectivity toward the formation of salicylic aldehyde is $>85\%$ (at 90% conversion) on gold catalysts supported on Fe_2O_3 and $CaCO_3$, while gold catalysts supported on Al_2O_3 and ZnO show a selectivity even higher than 90% at high conversion.
- It was suggested that on gold catalysts supported on Me_xO_y ($Me = Al(III), Zn(II), Fe(III)$) the active oxygen species are supplied by the oxygen lattice of the support, whereas the catalytic activity of gold supported on $CaCO_3$ can be ascribed to the enhancement of the reactivity of gold toward the activation of gaseous oxygen caused by the expansion of the metal lattice.

Acknowledgment

This work is part of a project coordinated by Prof. B. Corain and co-financed by the Italian MIUR (COFIN 01, Area 03).

References

- [1] M. Haruta and M. Daté, Appl. Catal. A: General 222 (2001) 427.
- [2] M. Shibata, N. Kawata, T. Masumoto and H. Rimura, J. Chem. Soc., Chem. Commun. (1988) 154.
- [3] J.E. Bailie and G.J. Hutching, Chem. Commun. (1999) 2151.
- [4] C. Mohr, H. Hofmeister, M. Lucas and P. Claus, Chem. Eng. Technol. 23 (2000) 324.
- [5] J.E. Bailie, H.A. Abdullah, J.A. Anderson, C.H. Rochester, N.V. Richardson, N. Hodge, J.G. Zhang, A. Burrows, C.J. Kiely and G.J. Hutching, Phys. Chem. Chem. Phys. 3 (2001) 4113.
- [6] C. Milone, M.L. Tropeano, G. Gulino, G. Neri, R. Ingoglia and S. Galvagno, Chem. Commun. (2002) 868.
- [7] L. Prati and M. Rossi, J. Catal. 176 (1998) 552.

- [8] C. Milone, R. Ingoglia, G. Neri, A. Pistone and S. Galvagno, Appl. Catal. A: General 211 (2001) 251.
- [9] K. Hamada and G. Suzukamo, US Patent 4,469,894 (1984).
- [10] K. Hamada and G. Suzukamo, US Patent 4,584,410 (1984).
- [11] L. Weisse, R. Neunteufel, B. Nenndorf and H. Strutz, US Patent 5,395,978 (1995).
- [12] J. Le Ludec, US Patent 4,026,950 (1977).
- [13] B. Kurt, M. Reiner, F. Helmut and W. Karlfried, US Patent 4,119,671 (1978).
- [14] H. Lanfranc, US Patent 5,689,009 (1997).
- [15] Y. Christidis and J.C. Vallejos, US Patent 4,481,374 (1984).
- [16] A. Wolf and F. Scüth, Appl. Catal. A: General 226 (2002) 1.
- [17] F.E. Wagner, S. Galvagno, C. Milone, A.M. Visco, L. Stievano and S. Calogero, J. Chem. Soc. Faraday Trans. 93 (1997) 3403.
- [18] G. Neri, A.M. Visco, S. Galvagno and M. Panzalorto, Thermochim. Acta 329 (1999) 39.
- [19] Y.J. Chen and C. Yeh, J. Catal. 200 (2001) 59.
- [20] L.I. Ilieva, D.H. Andreeva and A.A. Andreev, Thermochim. Acta 292 (1997) 169.
- [21] D. Andreeva, V. Idakiev, T. Tabakova, L. Ilieva, P. Falaras, A. Bourlino and A. Travlos, Catal. Today 72 (2002) 51.
- [22] S. Minicò, S. Scirè, C. Crisafulli, R. Maggiore and S. Galvagno, Appl. Catal. B: Environmental 34 (2001) 277.
- [23] Q.F. Adam Weber and M. Flytzani-Stephanopoulos, Catal. Lett. 77 (2001) 87.
- [24] S. Golunski, R. Rajaram, N. Hodge, G.H. Hutchings and C.J. Kiely, Catal. Today 72 (2002) 107.
- [25] J.C. Frost, Nature 334 (1988) 577.
- [26] R.R. Rajaram, J.W. Hayes, G.P. Ansell and H.A. Hatcher, US Patent 5,993,762 (1999).
- [27] Unpublished results.
- [28] M. Haruta, H. Kageyama, N. Kamijo, T. Kobayashi and F. Delannay, in: *Successful Design of Catalysts, Studies in Surface Science*, ed. T. Inui (Elsevier, Amsterdam, 1988) p. 33.
- [29] A.M. Visco, F. Neri, G. Neri, A. Donato, C. Milone and S. Galvagno, Phys. Chem. Chem. Phys. 1 (1999) 2869.
- [30] S. Minicò, S. Scirè, C. Crisafulli, A.M. Visco and S. Galvagno, Catal. Lett. 47 (1997) 273.
- [31] C.F. Baes Jr. and R.E. Mesmer, *The Hydrolysis of Cations* (Wiley, New York, 1976) p. 279.
- [32] M. Mavrikakis, P. Stolze and J.K. Nørskov, Catal. Lett. 64 (2000) 101.
- [33] K.H. Choi, B.Y. Coh and H.I. Lee, Catal. Today 44 (1998) 205.